J. T. GILLIS
Systems Research Center
University of Maryland
College Park, MD 20742

Author's current address:
The Aerospace Corp. M4/971
P.O. Box 92957
Los Angeles, CA 90009-2957

REFERENCES

[1] Arfken, G. B. (1985)
Mathematical Methods for Physicists (3rd ed.).
New York: Academic Press, 1985.

[2] Bender, C. M., and Orzag, S. A. (1978)
Advanced Mathematical Methods for Scientists and Engineers.
New York: McGraw-Hill, 1978.

[3] Lebedev, N. N. (1972)
Special Function & Their Application.
New York: Dover, 1972.

[4] Press, W. H., et al. (1988)
Numerical Recipes in C.
New York: Cambridge, 1988.

[5] White, R. G. (1975)
Distribution and moments of radial error.
Technical report NASA TM X-64962, NASA, 1975.

Estimation of 3-D Angular Motion Using Gyroscopes and Linear Accelerometers

This work presents a novel, real-time, angular motion estimation technique using a linear Gaussian estimator, and the outputs of linear accelerometers and gyroscopes, to assess the actual angular velocity of a rigid body in three-dimensional (3-D) space. The method obtains the covariances of the random actual 3-D angular velocity, the angular velocity measurement and the measurement noise, from the time averages of the outputs of an array of nine linear accelerometers and the outputs of three orthogonal gyroscopes. These statistics are used by the estimator to calculate the angular velocity of the rigid body in 3-D space. The multisensor technique performance is evaluated through a computer simulation. The results indicate the new method leads to more accurate angular velocity values than are obtained conventionally.

INTRODUCTION

Accurate knowledge of the angular motion of a vehicle is extremely important in many applications such as strap-down inertial navigation [1, 2], satellite and space vehicle attitude control [3, 4], fine pointing and tracking [5–7], inertial stabilization [8–10], long-range reconnaissance [11], and space photography [12]. Angular velocities are commonly measured using rate gyroscopes which are particularly sensitive to spurious torques acting on their gimbals leading to measurement noise [13, 14]. The magnitude of these random torques establishes the gyroscope noise level determining measurement uncertainty. To minimize this uncertainty, optimal estimators can be used.

The estimated state will, in general, be different from the actual or true state because of modeling errors and measurement noises. The goal of any estimation technique is to improve on the accuracy of the measuring device, so that the estimate is closer to the actual value than the measurement is. Enhanced performance is obtained at the expense of added complexity, but in many cases, this approach is more economical than using higher accuracy devices.

The optimal estimation of the angular velocity of a vehicle in three-dimensional (3-D) space, based on noisy gyro measurements, is an application of a more general problem of estimating the value of an unknown state vector from a related measurement vector. This has significant practical importance since an exact solution can be obtained.

Numerous estimation techniques have been developed to date [15–17]. These show that several of the major estimation algorithms lead to a common result for the linear and Gaussian case being considered here. However, to obtain angular velocity estimates based on data corrupted by noise, the statistics of both the process and the measurements need to be known. It is very unlikely that a complete ensemble of realizations from a random process would be accessible for the estimation process. In practice, time averages are used in place of ensemble averages, unless there is strong evidence to the contrary. This assumption is true for any ergodic process [18, 19]. Even when ergodicity is questionable, time averages still provide highly useful information, frequently the best available.

Consequently, this work presents a new method for obtaining the covariances of the actual 3-D angular velocity random process, the angular velocity measurement, and the measurement noise. These are obtained from the time averages of the outputs of an array of nine linear accelerometers and the outputs of three orthogonal gyroscopes. These statistics are then used with a linear-Gaussian estimator to assess the angular velocity of a rigid body in 3-D space. This constitutes the accelerometer gyro linear Gaussian (AGLG) estimation technique. The theory behind the development of this technique, and an evaluation of its performance, is presented in the following sections.

DYNAMICS OF RIGID BODIES IN 3-D SPACE

Before estimating the angular motion of a body, the basic equations governing its motion need to

Manuscript received January 8, 1991.

IEEE Log No. 9102989.

be understood. Kinematically, motion of a body can be explained geometrically by establishing the time-dependent relationships among its displacement, velocity, and acceleration. In so doing, it is frequently convenient to simultaneously use several frames of reference instead of a single inertial coordinate system. If one of these frames is designated as "fixed," the choice is arbitrary; the others, not rigidly attached to it, are designated as "moving."

Considering the two moving particles P and Q in Fig. 1, the vectors $\mathbf{R}_P$ and $\mathbf{R}_Q$ give the position of the two particles at any given time with respect to the fixed frame XYZ attached to O. The vector $\mathbf{R}_{Q/P}$ gives the position of Q relative to the moving frame $X'Y'Z'$ attached to P. Then it can be concluded that the position of Q is obtained by summing the vector $\mathbf{R}_{Q/P}$ to the vector $\mathbf{R}_P$. The change rate of these vectors is obtained by differentiation, defining the velocities $\mathbf{V}_Q$, $\mathbf{V}_P$ and $\mathbf{V}_{Q/P}$. A second differentiation gives the acceleration vectors $\mathbf{A}_Q$, $\mathbf{A}_P$ and $\mathbf{A}_{Q/P}$. This procedure leads to the well-known expression [20, 21] for the total acceleration of the particle Q (within the rigid body) with respect to an inertial coordinate frame attached to point O given below:

$$\mathbf{A}_Q = \mathbf{A}_P + \dot{\mathbf{W}} \times \mathbf{R}_{Q/P} + \mathbf{W} \times (\mathbf{W} \times \mathbf{R}_{Q/P}) \qquad (1)$$

where

$\mathbf{A}_P$ = acceleration of P with respect to O

$\dot{\mathbf{W}}$ = angular body acceleration

$\mathbf{W}$ = angular body velocity

$\mathbf{R}_{Q/P}$ = vector distance between P (start) and Q (end)

$\times$ = cross product operator.

Equation (1) shows that the most general motion of a rigid body is equivalent, at any given instant, to the sum of a translation (where all the body particles have the same acceleration as a reference particle P), and of a rotation (where the particle P is assumed to be fixed). Therefore, total acceleration measurements provide indirect information of the body angular motion. Padgaonkar, Hu, and others [22–26] have shown how to separate the accelerations due to translation from those due to rotation through various accelerometer placement schemes. They obtain expressions for angular acceleration measurements based on linear accelerometer outputs.

A past limitation of the technique has been its sensitivity to accelerometer cross-axis coupling effects [27]. However, newer accelerometer technology and manufacturing techniques have significantly reduced cross-axis sensitivity to less than a fraction of a percent in some devices; therefore, it is no longer a concern. Furthermore, recent developments in accelerometer technology have led to a new generation of solid-state devices that are smaller, lighter, more accurate and less expensive than their predecessors [28, 29]. These devices make measuring angular motion with linear accelerometers a cost-effective alternative to using angular sensors.

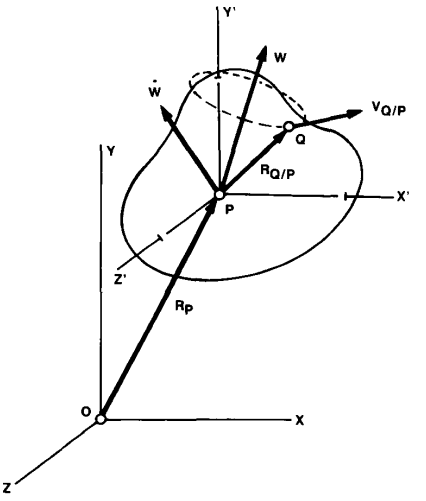

Fig. 1. Three-dimensional motion.

To illustrate how angular motion can be measured with linear sensors, consider the most general sensor arrangement shown in Fig. 2. Point O represents the center of vehicle rotation around which the angular velocity $\mathbf{W} = [W_X W_Y W_Z]^T$ is exerted. Tri-axial linear accelerometers are placed at points A, B, C, and D, providing the following 12 outputs: A_A^X, A_A^Y, A_A^Z, A_B^X, A_B^Y, A_B^Z, A_C^X, A_C^Y, A_C^Z, A_D^X, A_D^Y, and A_D^Z, where A_D^Z is the acceleration at point D in the Z direction, and likewise for the other outputs. Also, since the positions of each accelerometer with respect to each other ($\mathbf{R}_{B/A}, \mathbf{R}_{C/A}, \mathbf{R}_{D/A}$) are known, all the necessary data is readily available to extract the desired angular motion information. Substituting these values into (1), and expanding the acceleration equations for $\mathbf{A}_B$, $\mathbf{A}_C$, and $\mathbf{A}_D$ in the direction of each axis, the following identities result:

$$\begin{aligned} A_B^X &= [A_A^X - R_{B/A}(W_Y^2 + W_Z^2)] \\ A_B^Y &= [A_A^Y + R_{B/A}(\dot{W}_Z + W_X W_Y)] \\ A_B^Z &= [A_A^Z - R_{B/A}(\dot{W}_Y - W_X W_Z)] \end{aligned} \qquad (2)$$

$$\begin{aligned} A_C^X &= [A_A^X - R_{C/A}(\dot{W}_Z - W_X W_Y)] \\ A_C^Y &= [A_A^Y - R_{C/A}(W_X^2 + W_Z^2)] \\ A_C^Z &= [A_A^Z + R_{C/A}(\dot{W}_X + W_Y W_Z)] \end{aligned} \qquad (3)$$

$$\begin{aligned} A_D^X &= [A_A^X + R_{D/A}(\dot{W}_Y + W_X W_Z)] \\ A_D^Y &= [A_A^Y - R_{D/A}(\dot{W}_X - W_Y W_Z)] \\ A_D^Z &= [A_A^Z - R_{D/A}(W_X^2 + W_Y^2)]. \end{aligned} \qquad (4)$$

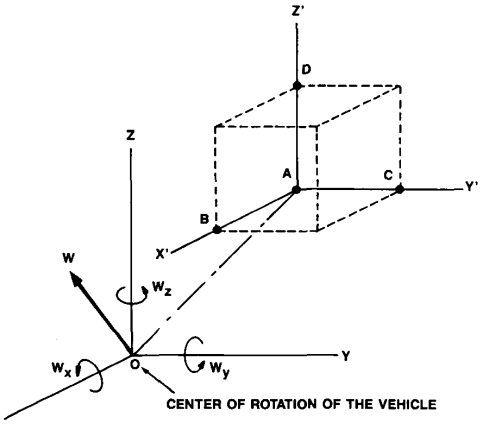

ANGULAR VELOCITY OF THE VEHICLE
$\underline{W} = [\,W_X\ W_Y\ W_Z\,]$

Fig. 2. Measuring linear accelerations.

The above system of equations (2)–(4) can be modified to obtain expressions for the angular accelerations, based on the outputs of the linear accelerometers (A_A^X through A_D^Z) for each of the orthogonal axes of a reference frame. This results in the new system of equations are given below:

$$\begin{aligned}\dot{W}_X &= (A_C^Z - A_A^Z)/2R_{C/A} - (A_D^Y - A_A^Y)/2R_{D/A}\\ \dot{W}_Y &= (A_D^X - A_A^X)/2R_{D/A} - (A_B^Z - A_A^Z)/2R_{B/A}\\ \dot{W}_Z &= (A_B^Y - A_A^Y)/2R_{B/A} - (A_C^X - A_A^X)/2R_{C/A}.\end{aligned} \tag{5}$$

Surprisingly, the importance of the additional information provided by the linear acceleration measurements, or how it can be used in the computation of the statistics of the angular motion, has been overlooked until now. This is seen by further manipulation of the initial system of equations (2)–(4), something that has not been done before, leading to the following equalities:

$$\begin{aligned}W_X W_Y &= (A_B^Y - A_A^Y)/2R_{B/A} + (A_C^X - A_A^X)/2R_{C/A}\\ W_X W_Z &= (A_B^Z - A_A^Z)/2R_{B/A} + (A_D^X - A_A^X)/2R_{D/A}\\ W_Y W_Z &= (A_C^Z - A_A^Z)/2R_{C/A} + (A_D^Y - A_A^Y)/2R_{D/A}\end{aligned} \tag{6}$$

$$\begin{aligned}W_X^2 &= (A_B^X - A_A^X)/2R_{B/A} - (A_C^Y - A_A^Y)/2R_{C/A}\\ &\quad - (A_D^Z - A_A^Z)/2R_{D/A}\\ W_Y^2 &= (A_C^Y - A_A^Y)/2R_{C/A} - (A_B^X - A_A^X)/2R_{B/A}\\ &\quad - (A_D^Z - A_A^Z)/2R_{D/A}\\ W_Z^2 &= (A_D^Z - A_A^Z)/2R_{D/A} - (A_B^X - A_A^X)/2R_{B/A}\\ &\quad - (A_C^Y - A_A^Y)/2R_{C/A}.\end{aligned} \tag{7}$$

Generally, it would be preferable to locate the accelerometers equidistantly. Then, $R_{B/A} = R_{C/A} = R_{D/A} = R$ and the above equations further simplify to:

$$\begin{aligned}W_X W_Y &= (A_B^Y - A_A^Y + A_C^X - A_A^X)/2R\\ W_X W_Z &= (A_B^Z - A_A^Z + A_D^X - A_A^X)/2R\\ W_Y W_Z &= (A_C^Z - A_A^Z + A_D^Y - A_A^Y)/2R\end{aligned} \tag{8}$$

$$\begin{aligned}W_X^2 &= (A_B^X - A_A^X - A_C^Y + A_A^Y - A_D^Z + A_A^Z)/2R\\ W_Y^2 &= (A_C^Y - A_A^Y - A_B^X + A_A^X - A_D^Z + A_A^Z)/2R\\ W_Z^2 &= (A_D^Z - A_A^Z - A_B^X + A_A^X - A_C^Y + A_A^Y)/2R.\end{aligned} \tag{9}$$

System of equations (8) gives the cross product of the angular velocities. System of equations (9) gives the square of the angular velocities. Notice how a measurement of the product of two angular velocities is obtained from a linear combination of the accelerometer outputs. This is a key result, because the time average of these signals provides, for ergodic motion, the correlation between the angular velocities needed to run the optimal estimators.

So far, the additive noise present in the accelerometers has not been taken into account. Making use of the additive noise model, the following relationships can be written for each accelerometer output:

$$\begin{aligned}A_A^X &= a_A^X + n_A^X\\ &\vdots\\ A_D^Z &= a_D^Z + n_D^Z\end{aligned} \tag{10}$$

where A is the measured acceleration, a is the actual acceleration, and n is the noise in the measurement.

Taking the expected value of these measurements, and assuming zero mean noise, the following is obtained:

$$\begin{aligned}E[A_A^X] &= E[a_A^X] + E[n_A^X] = E[a_A^X]\\ &\vdots \qquad\qquad \vdots\\ E[A_D^Z] &= E[a_D^Z] + E[n_D^Z] = E[a_D^Z].\end{aligned} \tag{11}$$

Making use of these equalities, the correlation of the actual angular velocities W_X, W_Y and W_Z, not the correlation of the measurements, is given by

$$\begin{aligned}E[W_X W_Y] &= E[a_B^Y - a_A^Y + a_C^X - a_A^X]/2R\\ E[W_X W_Z] &= E[a_B^Z - a_A^Z + a_D^X - a_A^X]/2R\\ E[W_Y W_Z] &= E[a_C^Z - a_A^Z + a_D^Y - a_A^Y]/2R\\ E[W_X^2] &= E[a_B^X - a_A^X - a_C^Y + a_A^Y - a_D^Z + a_A^Z]/2R\\ E[W_Y^2] &= E[a_C^Y - a_A^Y - a_B^X + a_A^X - a_D^Z + a_A^Z]/2R\\ E[W_Z^2] &= E[a_D^Z - a_A^Z - a_B^X + a_A^X - a_C^Y + a_A^Y]/2R.\end{aligned} \tag{12}$$

Furthermore, if the angular velocities are zero mean (or if the accelerometers have no dc response), the covariance matrix of W can be directly obtained by

proper ordering of these time averages as given below.

$$P_W = \text{cov}(\mathbf{W}) = E[\mathbf{W}\mathbf{W}^T] = \begin{vmatrix} E[W_X^2] & E[W_X W_Y] & E[W_X W_Z] \\ E[W_X W_Y] & E[W_Y^2] & E[W_Y W_Z] \\ E[W_X W_Z] & E[W_Y W_Z] & E[W_Z^2] \end{vmatrix} = P_X. \quad (13)$$

This is a very significant result because computing the state covariance matrix P_W in this manner leads to a more accurate value of the actual angular velocity covariance since the procedure is virtually immune to accelerometer measurement noise (zero mean noise is assumed). On the other hand, the approximation of P_W to the gyro measurement covariance matrix P_Z (as it is commonly done), which includes the noise, is only valid if the noise covariance is negligible when compared to that of the measurement. An additional advantage is that obtaining P_W through a linear combination of the accelerometer outputs, at the signal conditioning amplifier level, is computationally more efficient. This is because the multiplications between the angular velocities are avoided. The next section shows how to use this accurately computed actual angular velocity covariance (obtained from linear acceleration measurements) in conjunction with the angular velocity measurements from three orthogonal gyroscopes and an optimal linear Gaussian estimator, to assess the actual angular velocity of the body.

LINEAR GAUSSIAN ESTIMATION ALGORITHMS

The focus of this work is the real-time estimation of the 3-D angular velocity of a rigid body. To estimate any random variable, the probability distribution of the process that generated this variable needs to be known. It has been found through experience that the Gaussian distribution provides an accurate model for the behavior of many physical systems. In addition, this distribution provides an elegant analytical and computationally tractable form because its first and second moments, namely, its mean and covariance, completely specify the distribution. For the above reasons, the Gaussian distribution is selected here for modeling the random angular velocities of a rigid body.

Among the many estimation techniques currently available, several quickly stand out including the conditional mean, maximum likelihood, minimum variance, maximum a posteriori, and a few other estimators. It has been shown that several of the most popular estimation algorithms lead to a common result for the linear and Gaussian case (the one of primary interest in this work). The term "linear estimation" is used in the context that given a state vector $\mathbf{W}$ and a measurement vector $\mathbf{Z}$, the task of estimating $\mathbf{W}$ is performed with a linear operation on $\mathbf{Z}$. The state-measurement model is defined as follows:

$$\mathbf{Z} = H\mathbf{W} + \mathbf{V}. \quad (14)$$

Assuming the state $\mathbf{W}$ is Gaussian with mean $\mathbf{M}_W$ and covariance matrix P_W, and the measurement noise $\mathbf{V}$ is also Gaussian with mean $\mathbf{M}_V$ and covariance matrix P_V, the linear estimator $\mathbf{X}_E$ in its most complete form is given by

$$\mathbf{X}_E = [H^T P_V^{-1} H + P_W^{-1}]^{-1} \times [H^T P_V^{-1}(\mathbf{Z} - \mathbf{M}_V) + P_W^{-1}\mathbf{M}_W]. \quad (15)$$

Equation (15) shows that to compute the estimate $\mathbf{X}_E$, the first and second moments of the stochastic processes $\mathbf{W}$ and $\mathbf{V}$ need to be known. The statistics of the measurement noise vector, mean and covariance, could be premeasured under laboratory conditions. However, there is no guarantee that they will not change under different environmental and/or operating conditions. This creates uncertainty about the noise level present in the system at the time the angular motion measurements are taken. Statistics of the measurement $\mathbf{Z}$ can be calculated from the acquired data, and often, statistics of the actual state $\mathbf{W}$ are approximated to them for lack of a better term. However, the previous section shows that, in the case of angular motion, the actual angular velocity covariance could be obtained by linearly combining the accelerometer outputs and time averaging them. It also shows that this technique is virtually immune to accelerometer noise, obtaining a more accurate covariance value than that from gyroscope measurements. Furthermore, since the actual state covariance P_W can be obtained from accelerometers P_X, and the measurement covariance P_Z from gyroscopes, it follows that the noise covariance P_V can be inferred from the other two (assuming that $\mathbf{W}$ and $\mathbf{V}$ are uncorrelated) using the state-measurement model as follows:

$$P_V = P_Z - HP_X H^T. \quad (16)$$

Equation (16) provides the noise covariance based on current measurements and under the encountered operational environment. This leaves no doubt about the noise levels present in the measurements, and requires no previous covariance calculations and/or assumptions.

COMPUTER SIMULATION RESULTS

The AGLG technique performance was evaluated through a computer simulation using random motion as the test case maneuver. The actual angular velocity of the rigid body, represented by $\mathbf{W} = [W_X W_Y W_Z]^T$, was modeled to have band-limited Gaussian characteristics. Likewise, the angular velocity measurement vector $\mathbf{Z} = [Z_X Z_Y Z_Z]^T$, corresponding

to the outputs of the three orthogonal gyros (providing roll, pitch and yaw rates), were corrupted with band-limited white noise ($\mathbf{V} = [V_X V_Y V_Z]^T$). Lastly, the linear accelerometer outputs were also corrupted by zero mean Gaussian noise.

Band-Limited Random Variables

The band-limited Gaussian random variables corresponding to angular velocities and measurement noises were obtained using the Ornstein-Uhlenbeck algorithm. Generally, random number generators deliver a fixed total power (rms value), but the frequency spread depends on the calculation interval. For the purpose of this simulation, the low-frequency power density is of interest, and casual use of a random number generator into a low pass filter could lead to ill-defined variations. The Ornstein-Uhlenbeck process maintains a constant source of power over a specified frequency band (see [30]). The process is implemented by generating a correlated random sequence from the general formula:

$$N(i+1) = N(i)\exp(-T/\tau) + V(i) \tag{17}$$

where T is the sampling interval, τ is the correlation time constant, and V is a Gaussian random variable.

To find the $V(i)$ that produces the correct power P_N such that $E[N^2] = P_N$, (17) is squared, the expected value taken, and because it can be assumed that random variable V is uncorrelated with random variable N, the following relationship is obtained

$$E[N^2(i+1)] = E[N^2(i)]\exp(-2T/\tau) + E[V^2(i)]. \tag{18}$$

Making use of the following relationship:

$$E[N^2(i)] = E[N^2(i+1)] = P_N \tag{19}$$

$$E[V^2(i)] = (1 - \exp(-2T/\tau))P_N. \tag{20}$$

The band-limited random sequence generator can be expressed as

$$N(i+1) = N(i)\exp(-T/\tau) + P_N\sqrt{1-\exp(-2T/\tau)}G(i) \tag{21}$$

where $G(i)$ is a Gaussian random variable of zero mean and unit variance.

First Numerical Example

For this example, a low signal-to-noise ratio (SNR $\cong$ 1) condition is used (signal and noise have comparable magnitudes) to take advantage of the optimal estimator. In most applications, little is gained by using an estimator when the signal is much larger than the noise, or for that matter, when the noise is much larger than the signal. Also, to be able to visualize the random variable plots, the signal bandwidth is limited to 1 Hz. This is done by using the Orlstein-Uhlenbeck algorithm provided in the Advanced Continuous Simulation Language (ACSL) software (this is done for illustration purposes only, and should not be interpreted as a limitation of the technique). Thus, the normalized actual angular velocity random sequences have a 1-Hz bandwidth power spectral density, a standard deviation of one and zero mean. The measurement noise for the linear accelerometers is also modeled as a Gaussian random variable with zero mean and standard deviation of one, representing a SNR $\cong$ 1 condition. The record length is 1000 data points for each variable, covering a time span of 10 s of data acquired at a sampling rate of 0.01 s (the first 10 s of data are used for initialization).

The actual angular velocity covariance is defined as

$$P_W = E(\mathbf{W}\mathbf{W}^T) = \begin{vmatrix} P_W^{11} & P_W^{12} & P_W^{13} \\ P_W^{12} & P_W^{22} & P_W^{23} \\ P_W^{13} & P_W^{23} & P_W^{33} \end{vmatrix}. \tag{22}$$

Likewise, P_X is defined as the angular velocity covariance obtained from accelerometer data, P_Z as the angular velocity covariance obtained from gyroscope data, and P_V as the noise covariance in the gyroscope measurements.

Fig. 3 shows plots of the covariance elements versus time for P_W, P_X, P_V, and P_Z. These plots show that the standard deviation of matrix diagonal elements is not quite equal to one (nor equal to two in the case of P_Z). Also shown is some correlation between the orthogonal components of the motion. This is because of the limited bandwidth and the finite record length, and because the random generator did not output a truly Gaussian sequence. These data imperfections make the estimation example even closer to scenarios typically encountered in practice. Comparing P_Z to P_W shows that the former is roughly twice the latter; therefore, considering equal, as is commonly done in conventional estimation techniques, is not a good approximation. Conversely, P_X (from accelerometers) closely matches P_W (actual). Furthermore, the AGLG technique is the only presently available method that calculates the noise level in the angular velocity measurements as data has been acquired. This is very important for those cases where the additive noise may vary with time and/or operational conditions.

Even in this simulated case where data generation was tightly controlled, the noise covariance does not have the expected ideal characteristics given below

$$P_V = \begin{vmatrix} 1.0 & 0.0 & 0.0 \\ 0.0 & 1.0 & 0.0 \\ 0.0 & 0.0 & 1.0 \end{vmatrix}. \tag{23}$$

Finally, the results for the linear Gaussian estimation of angular velocities are given in Fig. 4. These show the actual angular velocity W (in roll, pitch

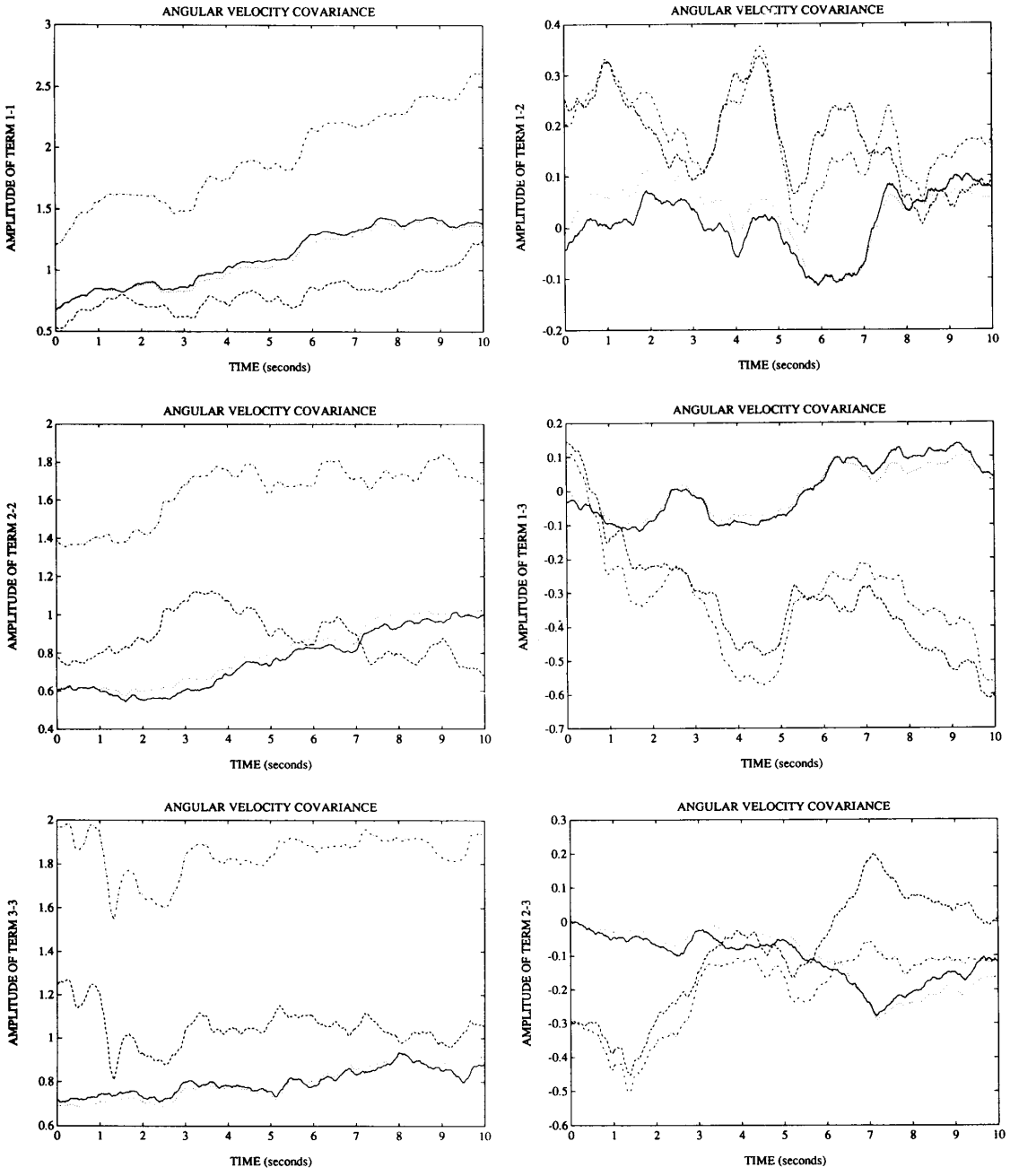

Fig. 3. Angular velocity covariances.

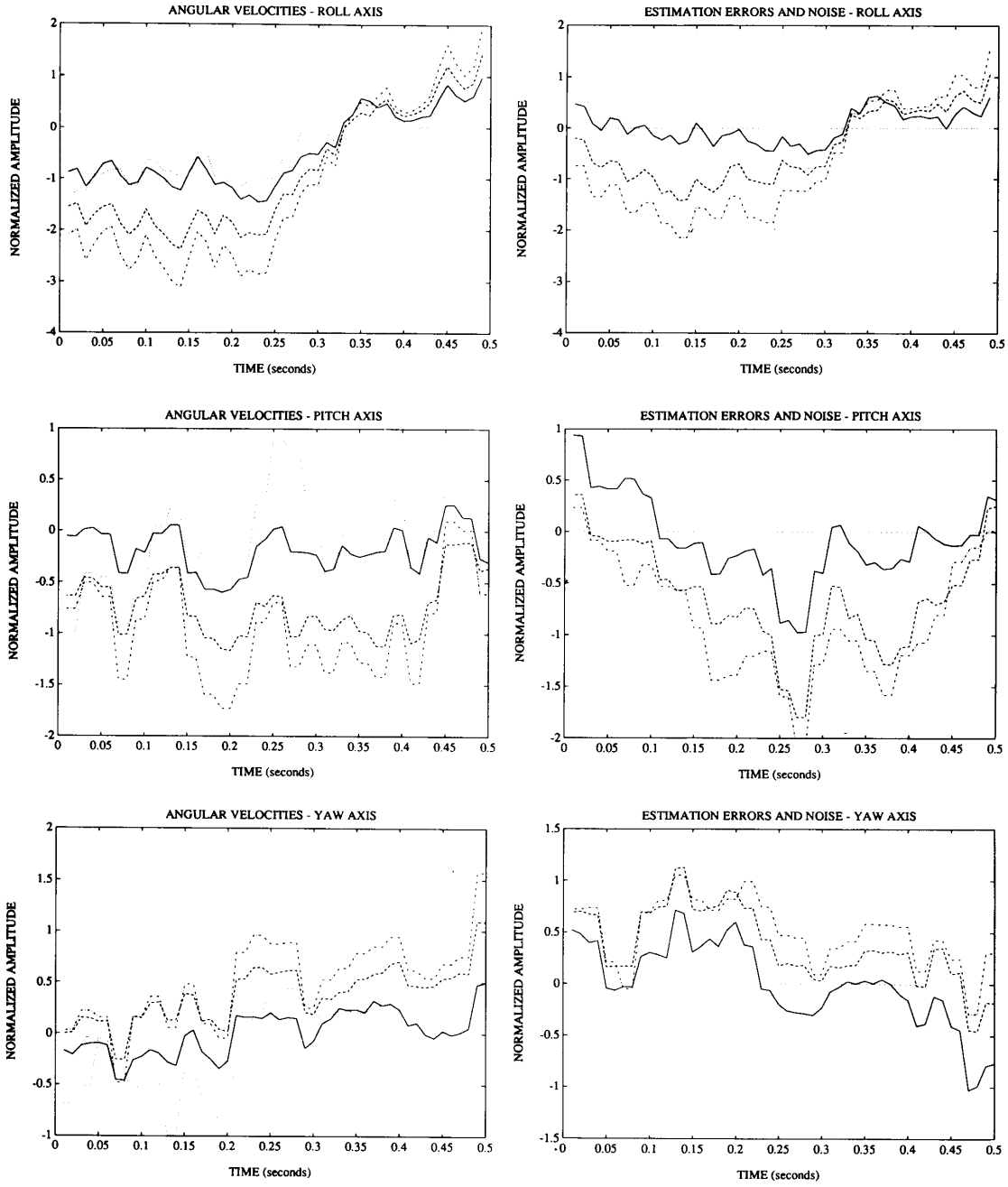

Fig. 4. Linear Gaussian estimation results.

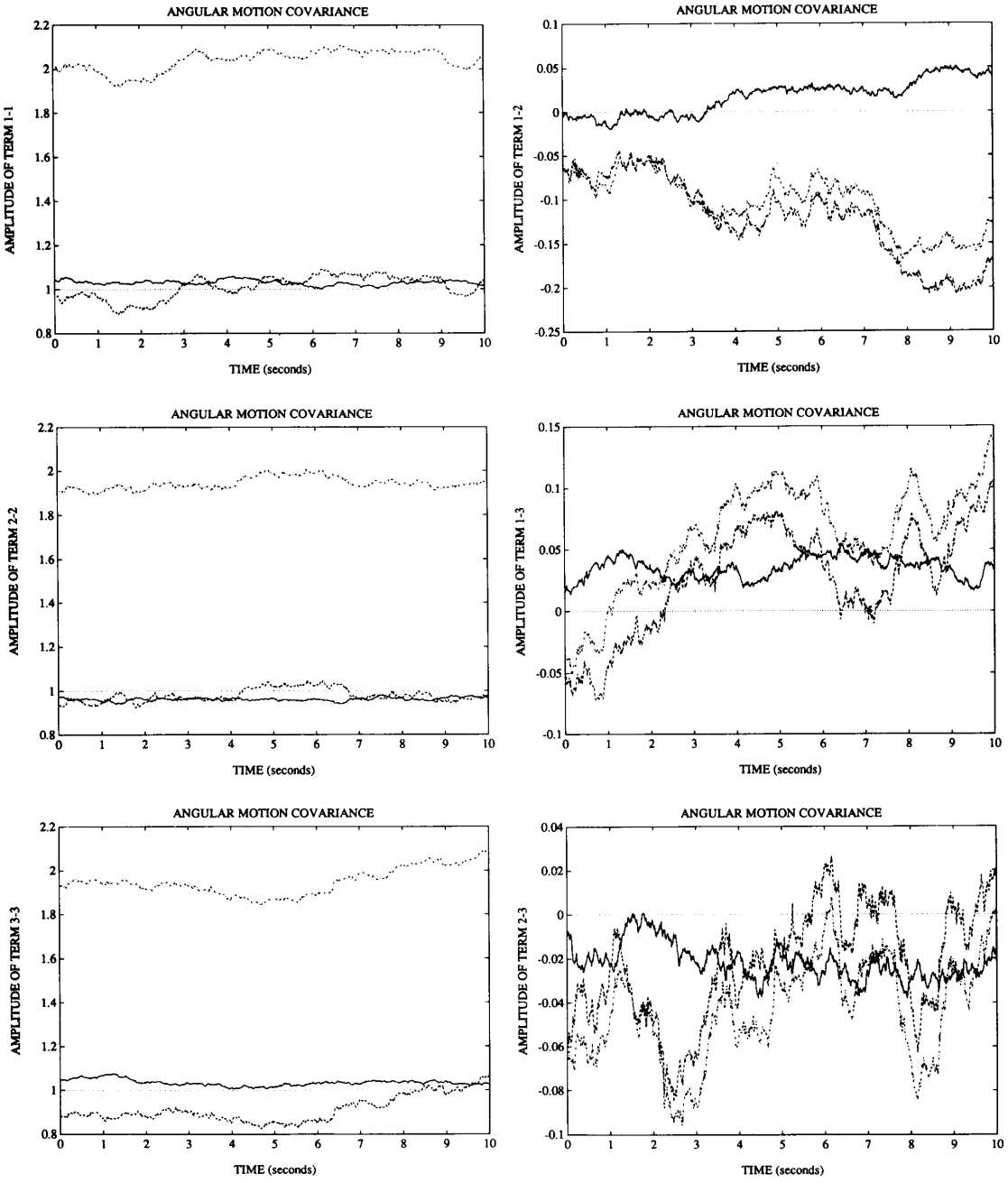

Fig. 5. Angular velocity covariances.

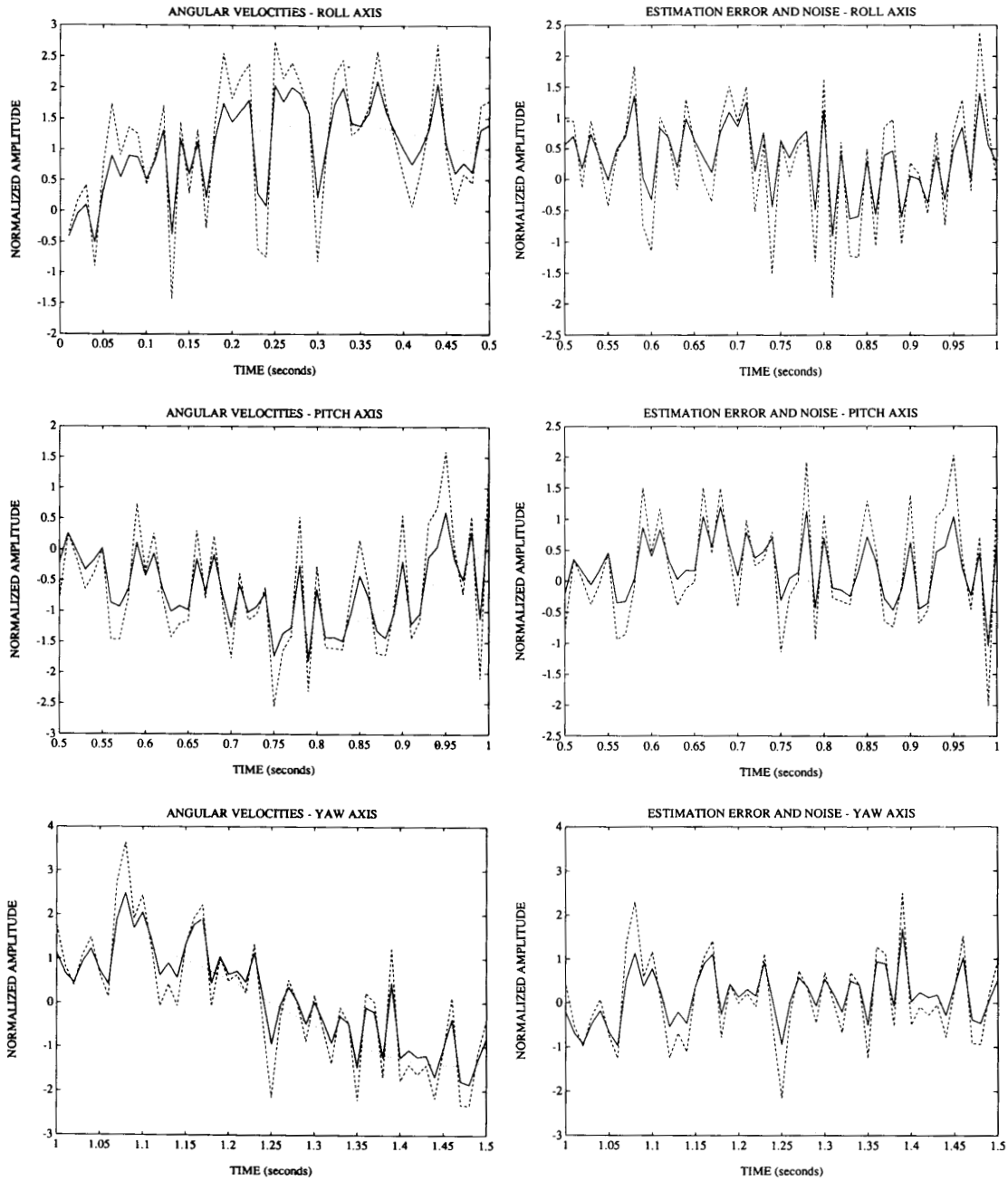

Fig. 6. Linear Gaussian estimation results.

TABLE I
MSE Values

	AGLG	Conventional	Measured
Roll Axis	0.4030	0.4540	0.7655
Pitch Axis	0.4840	0.5176	0.9210
Yaw Axis	0.4646	0.6408	1.2714

TABLE II
MSE Values

	AGLG	Conventional	Measured
Roll Axis	0.3870	0.5705	1.0832
Pitch Axis	0.3287	0.5009	0.9866
Yaw Axis	0.3763	0.5164	1.0101

and yaw), the AGLG estimate $\mathbf{X}_E$, the conventional estimate $\mathbf{X}_C$, the measurement $\mathbf{Z}$, the estimation errors for $\mathbf{X}_E$ and $\mathbf{X}_C$, and the noise $\mathbf{V}$. These results show that the AGLG technique consistently provides more accurate angular velocity values than the ones obtained from noise-corrupted gyroscope measurements and from conventional estimators. The mean square error (MSE) between the actual and estimated values, averaged over 1000 data points, is given in Table I. These MSE values clearly indicate that the AGLG technique provides reduction in mean square estimation error when compared with both conventional estimators and direct measurements.

Second Numerical Example

As a second numerical example, the AGLG technique is used to estimate the angular velocity of a rigid body undergoing the test maneuver with the following normalized angular rates ($\mathbf{W} = [W_X W_Y W_Z]^T$):

$$\begin{aligned} \text{Roll:}\quad & W_X(t) = \sqrt{2}\sin(2\pi f_R t) \quad \text{with} \quad f_R = 0.8 \text{ Hz} \\ \text{Pitch:}\quad & W_Y(t) = \sqrt{2}\sin(2\pi f_Y t) \quad \text{with} \quad f_Y = 1.0 \text{ Hz} \\ \text{Yaw:}\quad & W_Z(t) = \sqrt{2}\sin(2\pi f_Z t) \quad \text{with} \quad f_Z = 1.2 \text{ Hz}. \end{aligned} \tag{24}$$

The covariance of the above actual angular velocities is given by

$$P_W = E(WW^T) = \begin{vmatrix} 1.0 & 0.0 & 0.0 \\ 0.0 & 1.0 & 0.0 \\ 0.0 & 0.0 & 1.0 \end{vmatrix} \cong P_X. \tag{25}$$

The SNR is low (SNR $\cong$ 1), and Fig. 5 shows the plots of the covariance elements for P_W, P_X, P_V, and P_Z. The estimation results for this simulation are given in Fig. 6, showing the actual angular velocity $\mathbf{W}$, the AGLG estimate $\mathbf{X}_E$, the measurement $\mathbf{Z}$, the estimation error and the noise $\mathbf{V}$. The conventional estimate $\mathbf{X}_C$, which lies between the AGLG estimate technique and the measured value, is not shown to make the figures easier to interpret. Once again, the AGLG estimation technique provides consistently more accurate values for the 3-D angular velocity of the rigid body. This is also evident from the mean square estimation error values given in Table II.

SUMMARY AND CONCLUSIONS

This paper addresses the real-time estimation of rigid-body 3-D angular motion. The fundamental equations governing the motion are reviewed, and it is shown that the measurement of linear accelerations provides valuable information about body angular motion. An array of nine orthogonal linear accelerometers is used to sense the cross-product between angular velocities. The actual angular velocity covariance is computed from the time average of these signals, and it is shown that the procedure is virtually immune to noise in the acceleration measurements. The actual covariance (obtained from accelerometer data) can be subtracted from the measurement covariance (obtained from gyroscope data) to calculate the noise levels present in the angular velocity measurements under the encountered operating environment. Finally, the data from the multisensor system is processed by a linear Gaussian estimator to enhance the accuracy of the gyroscope angular velocity measurements.

Two numerical examples are given. The first for band-limited Gaussian motion, and the second for sinusoidal motion, both at low SNRs. In either case, the AGLG estimation technique consistently provides

more accurate values for the 3-D angular velocity of the rigid body, and lower mean square estimation errors.

MARCELO C. ALGRAIN
Dept. of Electrical Engineering
University of Nebraska-Lincoln
Lincoln, NE 68588-0511

JAFAR SANIIE
Dept. of Electrical and Computer Engineering
Illinois Institute of Technology
Chicago, IL 60616

REFERENCES

[1] Kayton, M., and Fried, W. (1969)
Avionics Navigation Systems.
New York: Wiley, 1969.

[2] Lechner, W. (1982)
Techniques for the development of error models for aided strapdown navigation systems.
AGARD report, Mar. 1982.

[3] Wolbers, H. L., and Woodworth, J. L. (1970)
Pointing and stability requirements for orbital experiments.
IEEE Transactions on Aerospace and Electronic Systems, **AES-6** (July 1970).

[4] Sandhu, G. S. (1974)
Rigid body pointing accuracy and stability criteria for an orbiting spacecraft.
AIAA Engineering Notes (Aug. 1974).

[5] Anderson, W. W., Groom, N. J., and Woolley, C. T. (1977)
The annular suspension and pointing system.
AIAA Conference Paper 78-1310, Aug. 1977.

[6] Walton, V. M. (1977)
Fine pointing control of orbiter-based gimballed payload.
AIAA Conference Paper 77-1091, Aug. 1977.

[7] Mohanty, N. C. (1980)
Two-axis gimballed sensor pointing error.
IEEE Conference Paper CH1554-5-1/80/0000-0653, Jan. 1980.

[8] Rue, A. K. (1969)
Stabilization of precision electro-optical pointing and tracking systems.
IEEE Transactions on Aerospace and Electronic Systems, **AES-5** (Sept. 1969).

[9] Baumann, J. L., Dixon, M. D., and Russell, D. W. (1979)
Analysis and simulation of an advanced inertial stabilization concept.
Presented at the IEEE Winter Simulation Conference, Dec. 1979.

[10] Forys, E. L. (1980)
Internal bearing stabilized sighting unit.
Presented at the SPIE Conference, San Diego, CA, July 1980.

[11] Lewis, G. R. (1989)
Image stabilization techniques for long range reconnaissance camera.
SPIE Paper TD-373-1, Aug. 1989.

[12] Bell, T. E.(1990)
The main event: Images from the Voyager II spacecraft.
IEEE Spectrum (Jan. 1990).

[13] Irvine, R. B., and Van Alstine, R. (1979)
Performance advantages of dynamically tuned gyroscopes in high accuracy spacecraft pointing and stabilization applications.
Presented at the Symposium on Gyro Technology, Stuttgart, Germany, Sept. 1979.

[14] Reddy, P. B. (1981)
Performance comparison of a dry tuned gimbal two-degree-of-freedom gyro and gas bearing gyros in precision attitude determination systems.
NAECON '81, May 1981, Dayton, Ohio.

[15] Meditch, J. S. (1969)
Stochastic Optimal Linear Estimation and Control.
New York: McGraw-Hill, 1969.

[16] Chui, C. K., and Chen, G. (1987)
Kalman Filtering with Real-Time Applications.
New York: Springer-Verlag, 1987.

[17] Sage, A. P., and White, C. C. (1977)
Optimum Systems Control (2nd ed.).
Englewood Cliffs, NJ: Prentice-Hall, 1977.

[18] Papoulis, A. (1984)
Probability, Random Variables, and Stochastic Processes (2nd ed.).
New York: McGraw-Hill, 1984.

[19] Stark, H., and Woods, J. (1986)
Probability Random Processes, and Estimation Theory for Engineers.
Englewood Cliffs, NJ: Prentice-Hall, 1986.

[20] Beer, F., and Johnson, E. (1984)
Vector Mechanics for Engineers (4th ed.).
New York: McGraw Hill, 1984.

[21] D'Souza, A. F., and Garg, V. K. (1984)
Advanced Dynamics, Modeling and Analysis.
Englewood Cliffs, NJ: Prentice-Hall, 1984.

[22] Padgaonkar, A. J., Krieger, K. W., and King, A. I. (1975)
Measurement of angular acceleration of a rigid body using linear accelerometers.
Transactions of the American Society of Mechanical Engineers, (Sept. 1975).

[23] Hu, A. S. (1977)
Rotational measurement techniques using linear accelerometers.
In *Proceedings of International Instrumentation Symposium*, Las Vegas, NV, May 1977.

[24] Schuler, A., Grammatikos, A., and Fegley, K. (1965)
Measuring rotational motion with linear accelerometers.
Presented at the IEEE Annual East Coast Conference on Aerospace and Navigational Electronics, Baltimore, MD, 1965.

[25] Krishnan, V. (1965)
Measurement of angular velocity and linear acceleration using linear accelerometers.
AIAA, Oct. 1965.

[26] Lopatin, V. I. (1967)
Measurement of angular velocity of aircraft by means of linear accelerometers.
Joint Publication Research Service, Washington, DC, Mar. 1967.

[27] Hu, A. S. (1980)
Angular acceleration measurement errors induced by linear accelerometer cross-axis coupling.
The Shock and Vibration Bulletin, **50**, 2 (Sept. 1980), 11–16.

[28] Galler, D., and Booth, A. (1989)
The shocking truth of accelerometer selection.
Machine Design (July 6, 1989).

[29] Allen, H. V., Terry, S. C., and Knutti, J. W. (1989)
Understanding silicon accelerometers.
Sensors Magazine, (Sep. 1989).

[30] Mitchell and Gauthier Associates (1990)
Advanced Continuous Simulation Language Manual.
Concord, MA: Mitchell and Gauthier Associates, 1990.